Photocatalytic Degradation of Trimethoprim on Doped Ti-Pillared Montmorillonite

Beatriz González[a], Raquel Trujillano[a], Miguel A. Vicente[a,*], Vicente Rives[a], Sophia A. Korili[b] and Antonio Gil[b]

[a] *GIR-QUESCAT, Departamento de Química Inorgánica, Universidad de Salamanca, 37008 Salamanca, Spain*

[b] *INAMAT-Departamento de Ciencias, Universidad Pública de Navarra, 31006 Pamplona, Spain*

* Corresponding author.

E-mail address: mavicente@usal.es (M.A. Vicente).

ABSTRACT

Montmorillonite pillared with titanium and doped with Cr^{3+} or Fe^{3+} has been tested for the photo-degradation of the antibiotic trimethoprim (trimethoxybenzyl-2,4-pyrimidinediamine) under different conditions, namely, in the dark or in UV light, with or without catalyst, finding excellent catalytic performance under photocatalytic conditions. The degradation by-products were preliminary analysed by mass spectrometry. The results suggested that the molecule broke in two halves, corresponding to its two existing rings. The process continued with the breakage of new fragments from the trimethoxybenzene half, these fragments later reacted with the methoxy groups in this part of the molecule, giving species with m/z values higher than that for the starting molecule, and with the breakage of new fragments.

Keywords: Doped pillared montmorillonite; Trimethoprim degradation; Photocatalysis; Degradation by-products; Mass Spectrometry.

1. Introduction

Industrial and technological development of society involves in many cases release of harmful substances to the environment. To study different methods of bioremediation, so that their release into the environment remains within acceptable limits has become necessary. Pillared clay minerals have properties that could be interesting alternatives considering their high exchange capacity, low permeability, swelling ability, chemical and mechanical stability, high specific surface area and relatively low price. Similarly, clay minerals can be used for the removal of hazardous substances, such as heavy metals, dyes, biocides or pharmaceuticals, including antibiotics, from aquatic systems (Ismadji et al., 2015).

Titanium dioxide is the most widely used photocatalyst, due to its low cost, chemical inertness, photostability and biocompatibility (Scheneider et al., 2014), being widely used in photocatalytic degradation of pollutants (Nakata and Fujishima, 2012; Barbosa et al., 2015). Montmorillonite belongs to the smectite group, and is able to adsorb cations because of its exchange capacity and high specific surface area (Lv et al., 2017). The intercalation of polyoxocations between the sheets of clay minerals and their subsequent calcination give rise to structures stable up to high temperatures. This process of pillaring allows the use of clay minerals as adsorbents and catalysts (Gil et al., 2010), clay minerals pillared with titanium even showing greater photoactivity than TiO_2 particles (Kočí et al., 2011). Other successful method for incorporating TiO_2 to clay minerals is the formation of nanocomposites, by precipitation, sol-gel, etc. The TiO_2-clay solids have been widely used for photocatalytic removal of contaminants, particularly by Fenton reactions,

50 although other conditions have been widely explored in the last years. Dyes have been the
51 most studied contaminants, although other contaminants have also been widely considered
52 (Ramírez et al., 2010; Szczepanik, 2017).

53 The large use of antibiotics causes an increase of drug levels in the environment
54 due to the high percentage of unmetabolized active ingredient that is excreted by the living
55 organism (30-90%) (Putra et al., 2009). As a result, bacteria are generating resistance to
56 them; for this reason, a large number of researchers have carried out studies on the
57 adsorption of antibiotics from water by using different clay minerals (Chang et al., 2009;
58 Molu and Yurdakoc, 2010; Liu et al., 2012; Yan et al., 2012; Wu et al., 2013; Zhang et al.,
59 2013; Sturini et al., 2015).

60 Trimethoprim ($C_{14}H_{18}N_4O_3$, TMP) is a bacteriostatic antibiotic derived from
61 trimethoxybenzylpyrimidine that belongs to a group of chemotherapeutic agents known as
62 inhibitors of dihydrofolate reductase, mainly used for the treatment of urinary tract
63 infections, although it is also used in acute attacks of chronic bronchitis, acute otitis media
64 in children and enterocolitis (Liu et al., 2017). TMP is not completely metabolised during
65 the therapeutic process, and about 80% is excreted in its pharmacologically active form (Ji
66 et al., 2016; Zhang et al., 2016). The concentration of TMP found in the aquatic
67 environment has been reported to be 660-710 μg/L (Hirsch et al., 1999), with values of
68 600-760 μg/L in a Swedish hospital sewage water (Lindberg et al., 2004), 120-160 μg/L in
69 East Aurora and Holland wastewater effluents (Batt and Aga, 2005), and 13-15 μg/L in US
70 streams (Kolpin et al., 2002). The presence of TMP in water, even at the level of traces,
71 poses risks for the aquatic ecosystem, due to its ecotoxicological effects on aquatic
72 organisms and the inhibition of the growth of freshwater microalgae. Adsorption of 0.14-
73 0.44 mmol of TMP per gram of montmorillonite has been reported (Bekçi et al., 2006).

In this work, the photocatalytic degradation of trimethoprim in aqueous solution was studied, catalysed by montmorillonite pillared with titanium and doped with Cr^{3+} or Fe^{3+}. Up to our best knowledge, pillared clay-based catalysts have not been used for the photodegradation of trimethoprim, and the degradation of this molecule under photocatalytic treatment using clay-based catalysts, namely bentonite and vermiculite, has been reported only in one previous article (Martínez-Costa et al., 2018).

2. Experimental

2.1. Source material

The clay mineral used in this work was a raw montmorillonite (Mt) from Cheto, Arizona, USA (supplied by The Clay Minerals Repository, reference code SAz-1). It was purified by dispersion–decantation, collecting the ≤2 µm fraction. Its cation exchange capacity was 0.67 meq/g, its basal value 13.60 Å and its BET specific surface area 49 m^2/g (González-Rodríguez et al., 2015).

2.2 Preparation of the solids

Preparation of Ti-pillared Mt was carried out by modifying the method reported by Lin et al. (1993), doping with Cr and Fe by addition of these elements, as trivalent cations, to the Ti-solution before polymerization (González-Rodríguez et al., 2015). These solids were denoted as MtTiCr and MtTiFe, respectively. The characterization of the solids and the adsorption of TMP by these materials have been already reported (González-Rodríguez et al., 2015; González et al., 2017, respectively). Montmorillonite was correctly pillared by Ti-polycations, and their polymerization was strongly affected by the dopant elements. Solids with high acidities were obtained, with specific surface areas close to 300 m^2/g (for the solids used in the present work, 300 m^2/g for the Fe-doped solid, 272 m^2/g for the Cr-

doped solid, and 80 m^2/g for natural montmorillonite, all calcined at 500ºC) (González-Rodríguez et al., 2015).

2.3 Photocatalysis and mass spectrometry

For the photodegradation reaction, an MPDS-Basic system from Peschl Ultraviolet, with a PhotoLAB Batch-L reactor and a TQ150-Z0 lamp (power 150 W), integrated in a photonCABINET was used. Its spectrum is continuous, with the mean peaks at 366 nm (radiation flux, ϕ 6.4 W) and 313 nm (ϕ 4.3 W). The reactor was vertically oriented and it was refrigerated by circulating cold water (Fig. S1). In each test, 750 mg of catalyst was added to 750 mL of a TMP solution (25 mg/L) in EtOH/H_2O (1:1 v/v) (this solvent was used due to the low solubility of TMP in water). The concentration of TMP (Sigma-Aldrich, ≥98% (HPLC)) in the solutions after reaction was determined by UV-visible spectroscopy, using a Thermo Electron Helios Gamma spectrophotometer. The absorption was measured at 288 nm, the wavelength corresponding to the maximum absorbance of TMP. The calibration at this wavelength showed that the absorbance had a linear response, according to the Beer-Lambert law, in the concentration range from 1 to 50 mg/L.

In order to determine the by-products generated during UV degradation, the solutions were analysed after various treatment times by mass spectrometry. The equipment used for this purpose was an Agilent 1100 HPLC coupled to an ultraviolet detector and an Agilent Trap XCT mass spectrometer. Identification and evaluation of the decomposition products were performed by mass spectrometry analysis, by direct injection of the samples and ionization by positive electrospray at a voltage of 3.5 kV. These analyses were carried out at Servicio Central de Análisis Químico, Cromatografía y Espectrometría de Masas (University of Salamanca).

3. Results and discussion

3.1 TMP photodegradation

The degradation experiments were carried out under different conditions. First, the experiment was carried out under UV-light but in absence of any catalyst (photolysis). The C/C_0 ratio (C=concentration at time *t*, C_0=initial concentration) has been plotted vs. reaction time (Fig. 1), showing that UV light degraded up to 37% of the antibiotic after 240 min reaction.

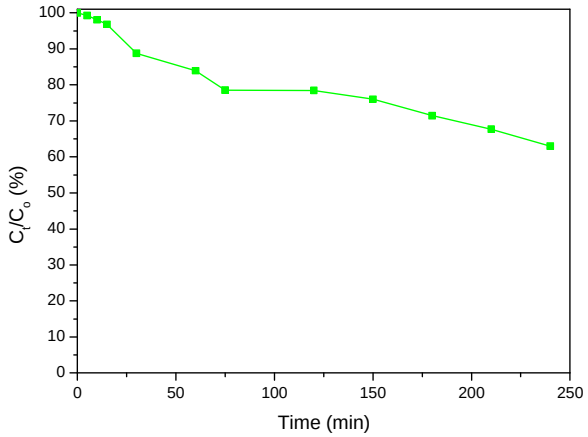

Fig. 1. Photolysis of TMP (degradation in the presence of UV-light and the absence of catalyst).

Degradation of TMP was studied in the presence of parent Mt and of the two doped-, Ti-pillared montmorillonites (Fig. 2). The degradation was studied in the darkness (left panel) and in the presence of UV light (right panel). In the darkness, the decrease in the concentration of TMP should be due to adsorption on the solids, allowing to compare with the true degradation caused in the presence of UV light.

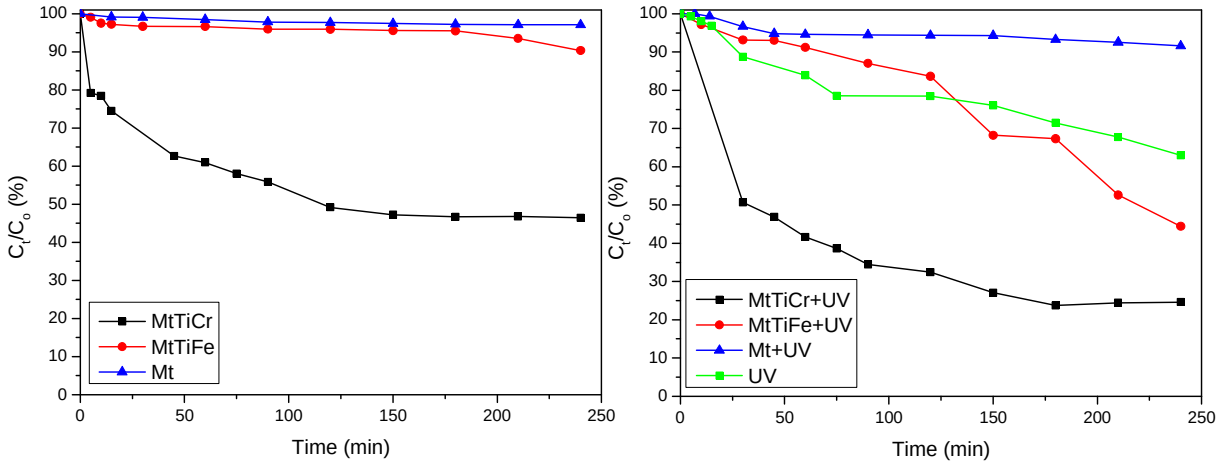

Fig. 2. TMP degradation in the darkness (left) and under UV irradiation (right), using parent Mt and the doped- Ti-pillared montmorillonites as catalysts. Photolysis results (with no catalyst) were included in the right panel for comparison.

Concerning the experiments carried out with no UV illumination (Fig. 2, left panel), a removal of approximately 50% was observed after 120 min, which was maintained for longer reaction times, for sample MtTiCr. This result was rather different from those obtained when using parent Mt, which showed a removal of TMP merely close to 2-3% even after 240 min reaction, proving that the treatment of the clay, and specially the presence of Cr, were key factors for the degradation. In the case of the solid doped with iron, adsorption may also dominate the process, although removal of TMP increased at longest times (180 minutes), suggesting that degradation also took place.

For the photocatalytic experiments, the degradation observed on Mt was lower than in the photolysis experiment. This may be explained by the turbidity of the dispersion induced by the presence of the catalyst. That is, the presence of montmorillonite hindered complete access of light to the dispersed particles, and this provoked degradation of the antibiotic to be lower than in the absence of catalyst. The sample doped with iron degraded

TMP in a lower amount than photolysis up to 125 min, also probably because of a turbidity effect, but degradation overcame photolysis at longer times, reaching 50% after 240 min. Again under these conditions, the sample doped with chromium showed the best behaviour, reaching a degradation of 76.3% after 180 minutes, and keeping constant for longest times. For a better observation of the degradation of TMP, the experiments carried out with each catalyst were compared (Fig. 3).

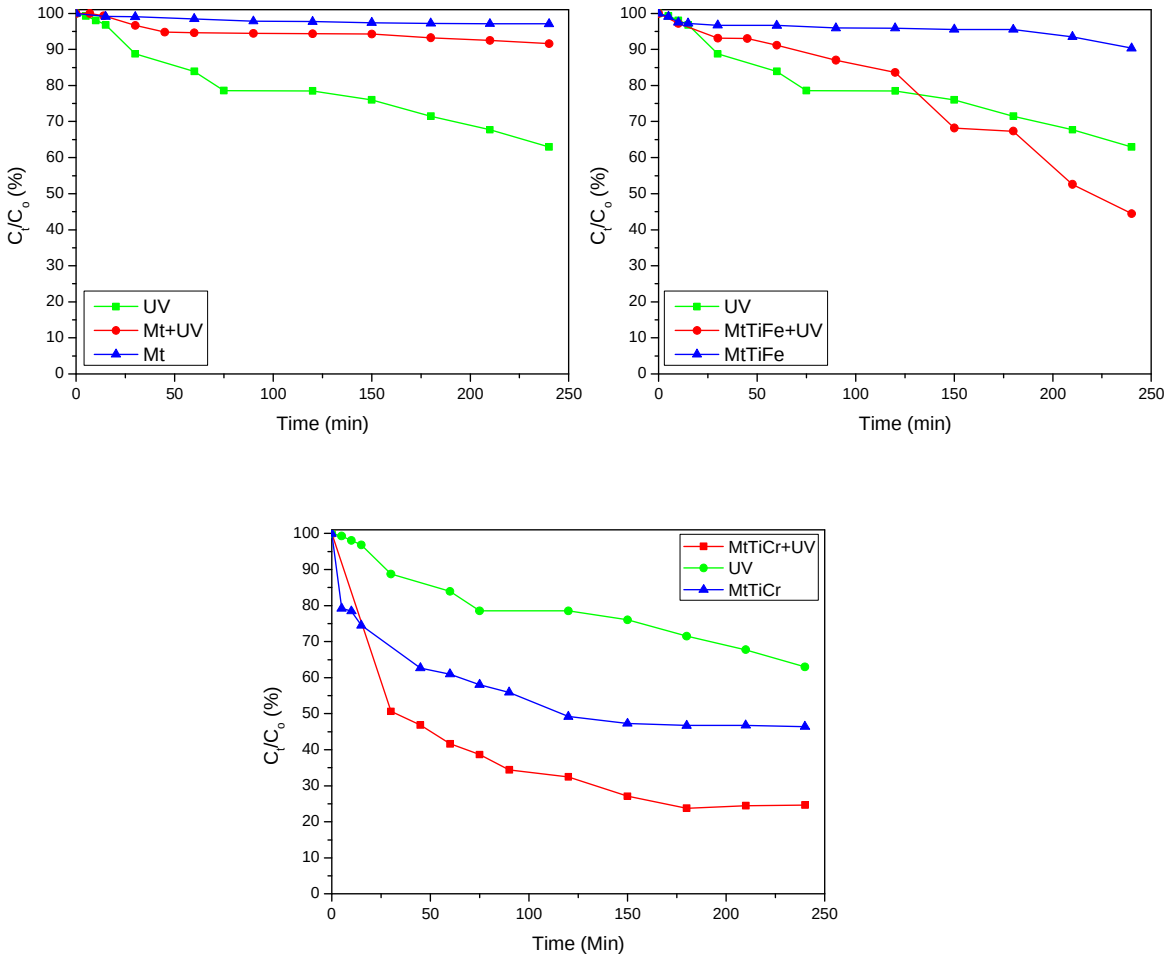

Fig. 3. Photodegradation of TMP for each of the catalyst under the different conditions tested: photolysis, in the presence of catalyst but in absence of UV light, and in the presence of catalyst and of UV light.

The possible leaching of the transition cations was not evaluated, but it should be considered that pillared clay minerals incorporating transition metal cations have been used

as catalysts in different oxidation reactions under harsh conditions, and their leaching was usually very low, even negligible (Galeano et al., 2014).

Martínez-Costa et al. (2018) have recently reported 55.1% of TMP photodegradation in a solution containing 40 ppm TMP using 10 mg of bentonite. Cai and Hu (2017) reported 98% and 84% photodegradation for 300 ppb and 1 ppm solutions, respectively, using 0.05 g/L P25 TiO_2 in a continuous photoreactor (and only 12% when the experiment was performed in the dark). Oros-Ruiz et al. (2013) deposited Au nanoparticles on TiO_2-P25 obtaining in this case 81% degradation after 300 minutes (54% if UV irradiation was suppressed). Even with the obvious difficulties for comparing very different reaction conditions, it can be concluded that the results obtained with the Cr-containing catalyst were comparable to the best results previously reported.

3.2 Mass spectrometry

Measurement of the TMP degradation by the catalysts might be affected by the presence in solution of the by-products formed, that is, the degradation can give rise to organic intermediates which may absorb in the same or very close range as TMP. The nature of the possible by-products was checked by mass spectrometry.

The mass spectrum of original TMP (Fig. 4) showed a single peak at m/z 291.3, which corresponded to protonated trimethoprim ($C_{14}H_{19}N_4O_3^+$) (Zhang et al., 2016). It is remarkable that the trimethoprim sample used in this study was extremely pure; Barbarin et al. (2002) found in their study a bromine analogue of TMP that should be formed during the synthesis of the antibiotic; the peak involving the presence of bromine was absent in our spectrum.

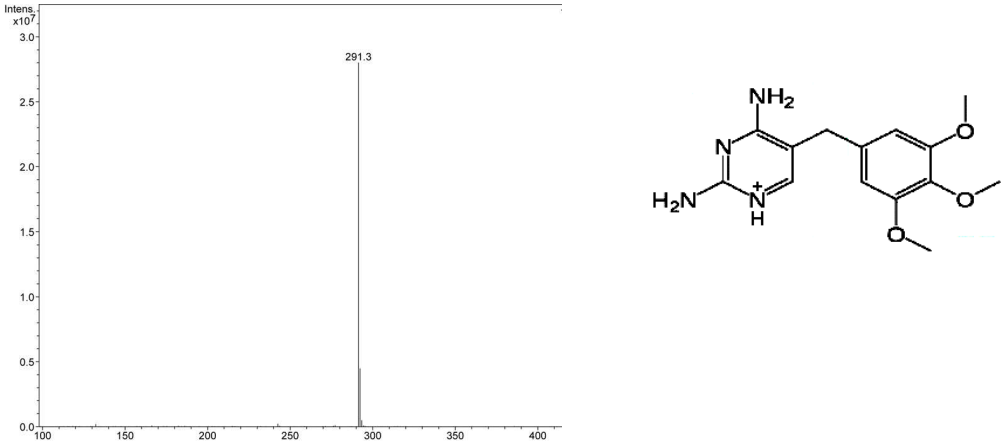

Fig. 4. Mass spectrum of the TMP (left) and formula of protonated TMP (right).

The spectra recorded after different degradation times using the best catalyst (MtTiCr) (Fig. 5 and Fig. S2, Supplementary material), evidenced the development of new peaks due to the degradation products. After degradation, the molecular peak was still recorded, and in addition new peaks with m/z ratios of 110, 185, 215, 242, 260, 277, 315, 337, 353, 381 and 433 were detected. The evolution of the intensity of the peaks with the photoreaction time was interesting (Fig. S3). For short photoreaction times, the molecular peak continued being the most intense one and, in addition, a relatively intense peak at m/z 242 was formed, followed by low intense peaks at larger m/z values than the molecular one. Then, the new peaks appeared and their intensities progressively increased, while the intensity of the molecular peak decreased one order.

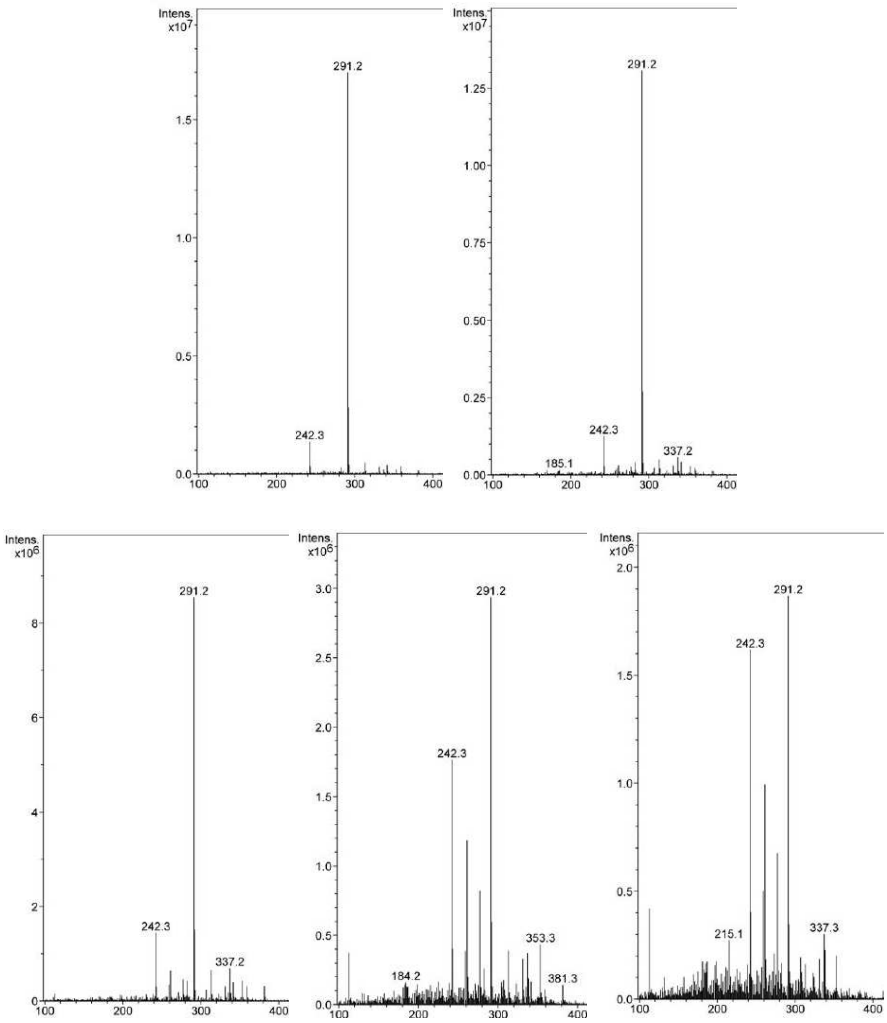

Fig. 5. Mass spectra of the reaction solution after different degradation times (15 (up, left), 30 (up, right), 75 (down, left), 180 (down, centre) and 210 (down, right) minutes, respectively) using MtTiCr as catalyst.

To analyse the possible degradation routes, the molecular structure of TMP can be split into two analogous substructures corresponding to 2,4-diaminopyridine (DAPD) and 1,2,3-trimethoxybenzene (TMBz) (Ji et al., 2016) (Fig. 6). The TMBz fragment, including the CH_2 bridging group, was found to appear at m/z 181 while the DAPD fragment was responsible of a signal at m/z 110.

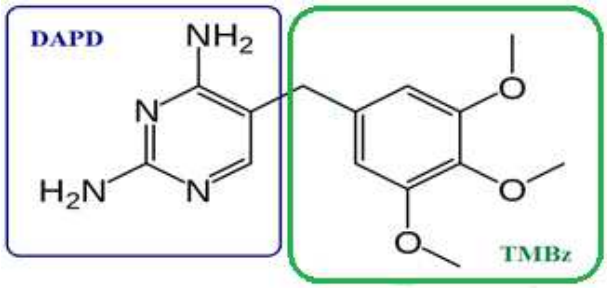

Fig. 6. Fragmentation of the molecular structure of TMP into two substructures.

From the development and changes in the intensities of the different peaks, it was evident that the first effect caused by photocatalysis was the formation of a fragment responsible for the peak at m/z 242 and almost simultaneously the peak at m/z 337 developed. The peak at 242 may correspond to the condensation between two adjacent methoxy groups forming ether (epoxide), which may elapse with the removal of C_2H_6 or, more probably, $\bullet CH_3$ or $CH_3O\bullet$ radicals (Barbarin et al., 2002; Eckers et al., 2005).

The mass loss by removal of a methoxy group (30 amu) and a –OH fragment (16 amu) was coincident with the mass gained by the fragment appearing at m/z 337 (46 amu) with respect to the molecular peak. This suggested that the groups initially broken from the TMP molecule can recombine with new molecules before being further degraded. Ethoxy and hydroxyl groups from the water:ethanol reaction medium may also participate in the reactions. Methoxy group in TMP can be substituted by larger groups, such as $CH_3CH_2COO–$, $CH_3COCH_2O–$ or $CH_3CH_2CH_2CH_2O–$, all of them giving rise to mass increases compatible with the values found (Barbarin et al., 2002). These routes were expected, since the hydroxyl radicals react preferentially via addition to carbon-carbon double bonds or by abstracting a proton from C–H, N–H or O–H units (Buxton et al., 1988; Pignatello et al., 2006). In addition, the TMBz fragment was more reactive for OH radicals than the DAPD fragment (Dodd et al., 2006).

At longer treatment times, smaller fragments appeared, mainly at m/z 184 and 110, as well as larger fragments, at m/z 315, 337, 353 and 381. The fragment at 110 has been assigned to the DAPD fragment of the original molecule (Barbarin et al., 2002; Eckers et al., 2005). The peak at 184 was close, although not coincident, to the mass of 182 assigned to the TMBz fragment of the molecule maintaining the bridging group (m/z 183). Other possibility would be the substitution of the terminal $–CH_3$ group of the molecule (once broken) by –OH, leading to a mass of 184, in agreement with the m/z 185, also detected in the spectra. The presence of fragments at m/z 315, 337, 353 and 381 suggested the incorporation of new groups to the molecule, probably chains previously broken from other molecules and/or groups from the solvents, groups that may be incorporated to the reactive methoxy groups in TMP. Other fragments, as those with m/z 277 or 215, have also been reported and explained elsewhere, assuming the DAPD fragment of the molecule, more stable, having different substituents (Barbarin et al., 2002; Eckers et al., 2005). Possible structures for these fragments were included in Table S1. As indicated, a discrepancy of 1-3 amu was found in some cases between the peaks now found and those reported in the literature.

The most complete studies on fragmentation of TMP were those from Barbarin et al. (2002) and Eckers et al. (2005). Barbarin et al. characterized the impurities and the degradation products existing in three commercial samples of TMP, while Eckers et al. studied the electrospray ionisation tandem mass spectrometry behaviour of trimethoprim and compounds with a similar structure containing alkoxy-phenyl groups. Eckers et al. (2002) found fragments at m/z 275, 261, 257 and 230 related to the reaction involving methoxy groups and/or their removal. The DAPD fragment gave rise to peaks at m/z 110 (the own DAPD fragment) and 123 (containing additionally the CH_2 group). Barbarin et al. (2005) reported two significant impurities in trimethoprim composition: in one of them,

one of the methoxy groups in the TMBz fragment was substituted by an ethoxy group, leading the molecular peak expected at 304, while in the other case one of the methoxy groups was substituted by a bromine atom, the molecular peak thus appearing at 338 and 340, according to the isotopes of this element (also chlorine may substitute the methoxy groups). These authors suggested that the DAPD fragment was rather stable, only one degradation route was suggested, with the removal of a H_2NCN moiety and formation of a four-membered ring (m/z 81), while the TMBz fragment showed a large number of parallel degradation routes, including the reaction of adjacent methoxy groups to form a cycle, the transformation of the methoxy groups into OH groups, the total removal of these groups, or the reaction of these groups with other outgoing fragments, among other possibilities.

Comparing our results with these reports, some of the fragments generated after photocatalysis were similar to those previously reported while, in other cases, the fragments were different. Considering the fragments found by mass spectrometry and the evolution of the intensities of their peaks with time, it can be proposed that the photodegradation of TMP followed a pathway similar to that found when this molecule was submitted to electrospray ionisation or in the own degradation of the molecule in commercial samples of this antibiotic, although the photocatalysis also produced new fragments not reported in previous studies. The general procedure seemed to be the breakage of fragments in the TMBz fragment of the molecule, with further reaction of these fragments with the own molecule, mainly with the very reactive methoxy groups, leading to species larger than the initial molecule, followed by further degradation steps. This mechanism, and also the toxicity of the intermediate species, would merit more detailed studies.

4. Conclusions

Titanium pillared montmorillonites, doped with Cr^{3+} or Fe^{3+} in the step of preparation of the pillaring solution, have been used as catalysts for the photo-degradation of the antibiotic trimethoprim. The solid doped with Cr^{3+} showed the best behaviour, with photodegradation close to 76% after 180 minutes of reaction. The degradation mechanism was investigated by mass spectrometry. The process seemed to include the breakage of the molecule in its two well-differentiated fragments, the trimethoxybenzene and diaminopyridine halves, the breakage of small fragments mainly from the trimethoxybenzene half of the molecule, the reaction of these fragments with the methoxy groups of other molecules giving to species larger than the initial molecule, and the subsequent breakage to new fragments.

Acknowledgments

The authors are grateful for financial support from the Spanish Ministry of Economy, Industry and Competitiveness (AEI/MINECO), and the European Regional Development Fund (ERDF) through grants MAT2013–47811–C2–R and MAT2016-78863-C2-2-R. BG thanks a pre-doctoral grant from Universidad de Salamanca.

Supplementary data

Supplementary data to this article can be found online at **********

5. References

Barbarin, N., Henion, J.D., Wu, Y., 2002. Comparison between liquid chromatography–UV detection and liquid chromatography–mass spectrometry for the characterization of impurities and/or degradants present in trimethoprim tablets. J. Chromatogr. A 970, 141–154.

Barbosa, L.V., Marçal, L., Nassar, E.J., Calefi, P.S., Vicente, M.A., Trujillano, R., Rives, V., Gil, A., Korili, S., Ciuffi, K.J., de Faria, E.H., 2015. Kaolinite–titanium oxide

nanocomposites prepared via sol–gel as heterogeneous photocatalysts for dyes degradation. Catal. Today 246, 133–142.

Batt, A.L., Aga, D.S., 2005. Simultaneous analysis of multiple classes of antibiotics by ion trap LC/MS/MS for assessing surface water and ground water contamination. Anal. Chem. 77, 2940–2947.

Bekçi, Z., Seki, Y., Yurdakoç, M.K., 2006. Equilibrium studies for trimethoprim adsorption on montmorillonite KSF. J. Hazard. Mater. 133, 233–242.

Buxton, G.V., Greenstock, C.L., Helman, W.P., Ross, A.B., 1988. Critical review of rate constants for reactions of hydrated electrons hydrogen atoms and hydroxyl radicals ($^{\cdot}OH/^{\cdot}O^{-}$) in aqueous solution. J. Phys. Chem. Ref. Data 17, 513–886.

Cai, Q., Hu, J., 2017. Decomposition of sulfamethoxazole and trimethoprim by continuous UVA/LED/TiO_2 photocatalysis: Decomposition pathways, residual antibacterial activity and toxicity. J. Hazard. Mater. 323, 527–536.

Chang, P.H., Li, Z., Yu, T.L., Munkhbayer, S., Kuo, T.H., Hung, Y.C., Jean, J.S., Lin, K.H., 2009. Sorptive removal of tetracycline from water by palygorskite. J. Hazard. Mater. 165, 148–155.

Dodd, M.C., Buffle, M.O., von Gunten, U., 2006. Oxidation of antibacterial molecules by aqueous ozone: moiety-specific reaction kinetics and application to ozone based wastewater treatment. Environ. Sci. Technol. 40, 1969–1977.

Eckers, C., Monaghan, J.J., Wolff, J.C. 2005. Fragmentation of Trimethoprim and other compounds containing a alkoxy-phenyl groups. Eur. J. Mass Spectrom. 11, 73–82.

Galeano, L.A., Vicente, M.A., Gil, A., 2014. Catalytic degradation of organic pollutants in aqueous streams by mixed Al/M-pillared clays (M = Fe, Cu, Mn). Catal. Rev. 56, 239–287.

Gil, A., Vicente, M.A., Korili, S.A., Trujillano, R., (Eds.), 2010. Pillared Clays and Related Catalysts.Springer, Heidelberg.

González-Rodríguez, B., Trujillano, R., Rives, V., Vicente, M.A., Gil, A., Korili, S.A., 2015. Structural, textural and acidic properties of Cu-, Fe- and Cr-doped Ti-pillared montmorillonites. Appl. Clay Sci. 118, 124–130.

González, B., Trujillano, R., Vicente, M.A., Rives, V., de Faria, E.H., Ciuffi, K.J., Korili, S.A., Gil, A., 2017. Doped Ti-pillared clays as effective adsorbents – Application to methylene blue and trimethoprim removal. Environ. Chem. 14, 267–278.

Hirsch, R., Ternes, T., Haberer, K., Kratz, K.L., 1999. Occurrence of antibiotics in the aquatic environment. Sci. Total Environ. 225, 109–118.

375 Ismadji, S., Soetaredjo, F.E., Ayucitra, A., 2015. Clay Materials for Environmental
376 Remediation. In: SpringerBriefs in Green Chemistry for Sustainability. Springer.
377 Ji, Y., Xie, W., Fan, Y., Shi, Y., Kong, D., Lu, J., 2016. Degradation of trimethoprim by
378 thermo-activated persulfate oxidation: Reaction kinetics and transformation
379 mechanisms. Chem. Eng. J. 286, 16–24.
380 Kočí, K., Matejka, V., Kovár, P., Lacny, Z., Obalová, L., 2011. Comparison of the pure
381 TiO_2 and kaolinite/TiO_2 composite as catalyst for CO_2 photocatalytic reduction. Catal.
382 Today 161, 105–109.
383 Kolpin, D.W., Furlong, E.T., Meyer, M.T., Thurman, E.M., Zaugg, S.D., Barber, L.B.,
384 Buxton, H.T., 2002. Pharmaceuticals, hormones, and other organic wastewater
385 contaminants in US streams, 1999–2000: a national reconnaissance. Environ. Sci.
386 Technol. 36, 1202–1211.
387 Lindberg, R., Jarnheimer, P.A., Olsen, B., Johansson, M., Tysklind, M., 2004.
388 Determination of antibiotic substances in hospital sewage water using solid phase
389 extraction and liquid chromatography/mass spectrometry and group analogue internal
390 standards. Chemosphere 57, 1479–1488.
391 Lin, J.T., Jong, S.J., Cheng, S., 1993. A new method for preparing microporous titanium
392 pillared clays. Microporous Mater. 1, 287–290.
393 Liu, N., Wang, M.X., Liu, M.M., Liu, F., Weng, L., Koopal, L.K., Tan, W.F., 2012.
394 Sorption of tetracycline on organo-montmorillonites. J. Hazard. Mater. 225–226, 28–
395 35.
396 Liu, L., Wan, Q., Xu, X., Duan, S., Yang, C., 2017. Combination of micelle collapse and
397 field-amplified sample stacking in capillary electrophoresis for determination of
398 trimethoprim and sulfamethoxazole in animal-originated foodstuffs. Food Chem. 219,
399 7–12.
400 Lv, P., Liu, C., Rao, Z., 2017. Review on clay mineral-based form-stable phase change
401 materials: Preparation, characterization and applications. Renew. Sust. Energ. Rev. 68,
402 707–726.
403 Martínez-Costa, J.I., Rivera-Utrilla, J., Leyva-Ramos, R., Sánchez-Polo, M., Velo-Gala, I.,
404 2018. Individual and simultaneous degradation of antibiotics sulfamethoxazole and
405 trimethoprim by UV and solar radiation in aqueous solution using bentonite and
406 vermiculite as photocatalysts. Appl. Clay Sci. 160, 217–225.

Molu, Z.B., Yurdakoc, K., 2010. Preparation and characterization of aluminum pillared K10 and KSF for adsorption of trimethoprim. Microporous Mesoporous Mater. 127, 50–60.

Nakata, K., Fujishima, A., 2012. TiO_2 photocatalysis: design and applications. J Photochem. Photobiol. Chem. 13, 169–189.

Oros-Ruiz, S., Zanellaa, R., Prado, B., 2013. Photocatalytic degradation of trimethoprim by metallic nanoparticles supported on TiO_2-P25. J. Hazard. Mater. 263, 28–35.

Pignatello, J.J., Oliveros, E., MacKay, A., 2006. Advanced oxidation processes for organic contaminant destruction based on the Fenton reaction and related chemistry. Crit. Rev. Environ. Sci. Technol. 36, 1–84.

Putra, E.K., Pranowo, R., Sunarso, J., Indraswati, N., Ismadji, S., 2009. Performance of activated carbon and bentonite for adsorption of amoxicillin from wastewater: mechanisms, isotherms and kinetics. Water Res. 43, 2419–2430.

Ramírez, J.H., Vicente, M.A., Madeira, M., 2010. Heterogeneous Photo-Fenton Oxidation with Pillared Clay-based Catalysts for Wastewater Treatment: A Review. Appl. Catal. B 98, 10–26.

Szczepanik, B., 2017. Photocatalytic degradation of organic contaminants over clay-TiO_2 nanocomposites: A review. Appl. Clay Sci. 141, 227–239.

Schneider, J., Matsuoka, M., Takeuchi, M., Zhang, J., Horiuchi, Y., Anpo, M., Bahnemann, D.W., 2014. Understanding TiO_2 photocatalysis: mechanisms and materials. Chem. Rev. 114, 9919–9986.

Sturini, M., Speltini, A., Maraschi, F., Rivagli, E., Pretali, L., Malavasi, L., Profumo, A., Fasani, E., Albini, A., 2015. Sunlight photodegradation of marbofloxacin and enrofloxacin adsorbed on clay minerals. J. Photochem. Photobiol. A 299, 103–109.

Wu, Q., Li, Z., Hong, H., 2013. Adsorption of the quinolone antibiotic nalidixic acid onto montmorillonite and kaolinite. Appl. Clay Sci. 74, 66–73.

Yan, W., Hu, S., Jing, C., 2012. Enrofloxacin sorption on smectite clays: effects of pH, cations, and humic acid. J. Colloid Interface Sci. 372, 141–147.

Zhang, Q., Yang, C., Huang, W., Dang, Z., Shu, X., 2013. Sorption of tylosin on clay minerals. Chemosphere 93, 2180–2186.

Zhang, Y., Wang, A., Tian, X., Wen, Z., Lu, H., Li, D., Li, J., 2016. Efficient mineralization of the antibiotic trimethoprim by solar assisted photoelectro-Fenton process driven by a photovoltaic cell. J. Hazard. Mater. 318, 319–328.